

This document is confidential and is proprietary to the American Chemical Society and its authors. Do not copy or disclose without written permission. If you have received this item in error, notify the sender and delete all copies.

**Investigation on Ash Slagging Characteristics during Combustion of Biomass Pellets and Effect of Additives**

|                               |   |
|-------------------------------|---|
| Journal:                      | <i>Energy &amp; Fuels</i>   |
| Manuscript ID                 | ef-2017-03173u  |
| Manuscript Type:              | Article   |
| Date Submitted by the Author: | 15-Oct-2017   |
| Complete List of Authors:     | Wang, Liang; SINTEF Energy Research, Thermal Energy Skjevrak, Geir; Norwegian University of Science and Technology Skreiberg, Øyvind; SINTEF Energy Research, Nielsen, Henrik; University of Agder, Department of Engineering Hustad, Johan; Norwegian University of Science and Technology, Department of Energy and Process Engineering Wu, Hongwei; Curtin University, Department of Chemical Engineering; Curtin University, Energy & Fuels |
|                               |   |

SCHOLARONE™  
Manuscripts

1  
2  
3  
4  
5  
6  
7  
8  
9  
10  
11  
12  
13  
14  
15  
16  
17  
18  
19  
20  
21  
22

# Investigation on Ash Slagging Characteristics during Combustion of Biomass Pellets and Effect of Additives

23  
24  
25  
26  
27

*Liang Wang*<sup>a,\*</sup>, *Geir Skjevrak*<sup>b</sup>, *Øyvind Skreiberg*<sup>a</sup>, *Hongwei Wu*<sup>c</sup>, *Henrik Kofoed Nielsen*<sup>d</sup>,  
*Johan E. Hustad*<sup>b</sup>

28  
29  
30  
31

<sup>a</sup> SINTEF Energy Research, Postboks 4761 Torgarden, Trondheim, Norway

32  
33  
34  
35  
36

<sup>b</sup> Department of Energy and Process Engineering, Norwegian University of Science and  
Technology, NO-7491, Trondheim, Norway.

37  
38  
39  
40  
41

<sup>c</sup> Department of Chemical Engineering, Curtin University, GPO Box U1987, Perth WA 6845,  
Australia

42  
43  
44  
45  
46  
47

<sup>d</sup> University of Agder, Department of Engineering Sciences, P.O. Box 509, NO-4898 Grimstad,  
Norway.

48  
49  
50  
51  
52  
53

\*Corresponding author. E-mail address: liang.wang@sintef.no;

54  
55  
56  
57  
58  
59  
60

Tel.: +47 48064531

1  
2  
3  
4  
5  
6 **ABSTRACT.** This study reports a systematic investigation into ash slagging behaviour during  
7  
8 combustion of barley straw and barley husk pellets with or without additives in a residential pellet  
9  
10 burner. The slagging tendencies of the pellets were evaluated based on the amount, chemistry,  
11  
12 mineralogy and morphology of inlet ash formed as slag and sintering degrees of residual ash. The  
13  
14 barley straw and husk pellets showed high slagging tendencies with 39 wt % and 54 wt % ingoing  
15  
16 ash formed as slag. Analyses using X-ray fluorescence (XRF) and scanning electron microscopy  
17  
18 combined with Energy-dispersive X-ray spectroscopy (SEM/EDX) revealed high concentrations  
19  
20 of K, Si, Ca but minor amount of P in barley straw slag. The slag mainly contained melted  
21  
22 potassium silicates, directly observed by X-ray diffraction (XRD). For the barley husk, high ash  
23  
24 slagging tendency was observed, mainly attributed to the formation and melting of potassium  
25  
26 phosphates, potassium silicates and complex mixtures of the two mineral phases. Addition of  
27  
28 marble sludge completely eliminated ash slagging during combustion of barley straw and husk  
29  
30 pellets because it led to the formation of high temperature melting calcium potassium phosphates,  
31  
32 calcium rich potassium silicates and oxides. Addition of calcium lignosulfonate showed a less  
33  
34 pronounced ability to mitigate ash slagging issues during pellets combustion, although it promoted  
35  
36 the formation of calcium rich silicates and phosphates (both with high-melting points) in barley  
37  
38 straw and husk ash, respectively. This process was accompanied by considerable reduction in the  
39  
40 amount and sintering degree of the formed barley straw and husk slag.  
41  
42  
43  
44  
45  
46

47  
48 **KEYWORDS:** Biomass pellets, combustion, ash slagging, additives  
49  
50  
51  
52  
53  
54  
55  
56  
57  
58  
59  
60

## 1 INTRODUCTION

Utilization of agricultural and food processing wastes for energy purpose has attracted continuous attention in the past decades. It is increasingly important in response to the increasing energy demand, limited availability of stem wood assortment and great need for disposing these solid waste materials.<sup>1</sup> However, the use of agricultural and food processing wastes for energy applications is not straightforward. These fuels inherently often have undesired properties such as high moisture content, low energy and bulk density, diverse particle sizes and shapes.<sup>2</sup> Most of these drawbacks can be improved and/or overcome through pelletization. In contrast to the raw materials, the pellets produced from agricultural and food processing wastes have lower moisture contents and more uniform, consistent and standardized properties as solid fuel, resulting in better ignition/combustion behaviors and thereby higher energy efficiency and lower emission during combustion processes.<sup>3</sup> The increased volume and energy density reduces costs for transport and storage, while the uniform dimensions makes handling and feeding of biomass pellets easier and more controllable. Pellets of agricultural and food processing wastes are suitable for many industrial and residential applications, e.g. combustion in burners and grate furnaces.<sup>4</sup>

However, combustion of pellets prepared from agricultural and food processing wastes in small to medium scale combustion appliances may face challenges from ash sintering and slagging that interfere combustion processes, reduce combustion stability and decrease energy conversion efficiency consequently.<sup>5,6</sup> The agricultural and food processing wastes often have high contents of ash forming matters, which can be 5-10 times of those of conventional woody biomass fuels.<sup>5</sup> Previous combustion experiments in residential combustion appliances showed that biomass fuels with high ash sintering and slagging tendency often contain large amounts of ash forming compounds.<sup>7-11</sup> Additionally, agricultural and food processing wastes contain abundant key ash-

1  
2  
3  
4  
5  
6 forming matters (i.e., K, Si, P and Ca) which are also more heterogeneous than those in woody  
7  
8 biomasses.<sup>12</sup> A general trend is that large amount of K and/or P can be found in agricultural and  
9  
10 food processing wastes, together with other main ash-forming elements like Si and Ca.<sup>13-15</sup>  
11  
12 Different than woody biomasses, relative concentrations of key ash forming elements (i.e., K, Si,  
13  
14 P and Ca) vary significantly for agricultural and food processing wastes.<sup>16-18</sup> It was reported that  
15  
16 the content of phosphorus in some agricultural wastes is even higher than that of silicon.<sup>13, 17</sup>  
17  
18 Therefore, in addition to silicates, different phosphates are formed readily and have been  
19  
20 observed in the ash residues from combustion of agricultural and food processing wastes.<sup>8, 13</sup>  
21  
22 Moreover, modes of occurrence of these elements in feedstock and ash have substantial effects on  
23  
24 ash transformation reactions and amount/properties of formed ash residues.<sup>17, 19, 20</sup> Extensive  
25  
26 chemical fractionation analyses for a wide range of biomass fuels showed that the association of  
27  
28 **ash forming matters** in agricultural and food wastes is considerably different from that of other  
29  
30 biomass fuels.<sup>17, 21</sup> The major fraction of K, Na and P in agricultural and food processing wastes  
31  
32 are present as water-soluble salts or organic-bound forms.<sup>17</sup> These ash-forming elements with high  
33  
34 solubility readily release during combustion and are active for further reactions to form compounds  
35  
36 that initiate different ash related operational problems.<sup>5, 19, 20</sup> Predictions based on chemical  
37  
38 fractionation analysis suggest that melting properties of ashes derived from agricultural and food  
39  
40 processing wastes correlate well with the high content of soluble ash-forming elements in the  
41  
42 feedstock.<sup>17, 20</sup> This correlation was also confirmed by experiments in combination with  
43  
44 thermodynamic equilibrium calculations.<sup>22</sup> Due to the specific ash characteristics, ash sintering and  
45  
46 slagging occur more often during the combustion of agricultural and food processing wastes. A  
47  
48 previous study reported that up to 80% of the fuel ash entering the burner ended up as slag after  
49  
50 the combustion of wheat straw.<sup>10</sup> For the combustion of cereal grains rich in phosphorus, 10-28%  
51  
52 of incoming fuel ash formed slag.<sup>8</sup> These slags are often completely fused ash in the form of large  
53  
54  
55  
56  
57  
58  
59  
60

1  
2  
3  
4  
5  
6 solid and hard blocks. Therefore, ash slagging causes great difficulties for achieving an efficient  
7  
8 and clean combustion of pelletized agricultural and food processing wastes and hinders further  
9  
10 utilization of such abundant biomass resources.

11  
12  
13 Utilization of additives is a promising and efficient way to abate ash sintering and slagging during  
14  
15 combustion of biomass pellets.<sup>23</sup> Several studies investigated slagging characteristics and effect of  
16  
17 additives during combustion of biomass pellets. Kaolin was found to be an efficient additive in  
18  
19 different studies for eliminating or significantly reducing ash slag formation during biomass pellets  
20  
21 combustion.<sup>7, 9, 24</sup> The kaolin chemically captures potassium compounds via different reaction  
22  
23 routes, reducing the amount of potassium available for forming potassium silicates that have low-  
24  
25 melting points.<sup>9</sup> As a consequence of this, both amounts of formed ash melts and ash slagging are  
26  
27 reduced. However, utilization of additives like kaolin is not financially attractive because of  
28  
29 relatively high costs. Different calcium-based additives were examined, including lime, limestone,  
30  
31 and calcite.<sup>8, 13, 24, 25</sup> For the combustion of biomass fuel rich in silicon, potassium and calcium and  
32  
33 with low content of phosphorus, addition of calcium leads to the formation of calcium rich silicates  
34  
35 and oxides (both having high melting points) in the ash residues.<sup>7, 25</sup> This is accompanied by partial  
36  
37 or even total elimination of ash sintering and slagging during combustion of these phosphorus-poor  
38  
39 biomass fuels. On the other hand, addition of calcium based additives altered the ash chemistry and  
40  
41 promoted the formation of potassium calcium phosphates that have high melting points as  
42  
43 phosphorus rich biomass fuels were burned in various combustion appliances.<sup>8, 10</sup> This is  
44  
45 considered as a main reason for the reduction in slag formation during the combustion of  
46  
47 phosphorus rich biomass fuels. It is desirable to explore additive candidates from waste resources,  
48  
49 which are available in a large amount at a relative low cost.<sup>6, 26</sup> In our previous work, addition of  
50  
51 marble sludge, a waste from the marble refining process, eliminated slag formation during the  
52  
53  
54  
55  
56  
57  
58  
59  
60

1  
2  
3  
4  
5  
6 combustion of wood waste in a residential boiler.<sup>25</sup> This was mainly attributed to the reduced  
7  
8 formation of alkali silicates (having low melting points), to more the increased formation of  
9  
10 calcium rich alkali silicates (having high melting points) in ash residues.<sup>25</sup> However, the effect of  
11  
12 marble sludge on ash slagging behavior during the combustion of agricultural and food processing  
13  
14 wastes have not been well understood. The calcium rich additive can also be found in waste streams  
15  
16 from the paper and pulp production process, in which significant amount of calcium carbonate is  
17  
18 used. In this work, calcium lignosulfonate derived from a paper and pulp production plant was  
19  
20 investigated. Calcium and sulfur are two dominating chemical elements of the calcium  
21  
22 lignosulfonate. From the ash chemistry point of view, these two elements are favorable for  
23  
24 mitigating ash related operational problems. However, no systematic study about the effect of  
25  
26 calcium lignosulfonate on slagging behaviors of biomass ash have been reported.  
27  
28  
29  
30

31  
32 The objectives of this work are to: i) investigate ash and slag forming processes during the  
33  
34 combustion of barley straw and barley husk pellets and; ii) evaluate the effect of marble sludge and  
35  
36 calcium lignosulfonate on slagging tendency and characteristics of the two fuels.  
37  
38  
39

## 40 2 MATERIALS AND METHODS

### 41 2.1 Fuels and Additives

42  
43  
44 Two biomass fuels, i.e. barley straw and barley husk, were used in the experimental program. The  
45  
46 barley straw was harvested in the county Hedmark in Norway and then stored indoors properly, in  
47  
48 order to avoid further degradation and loss of water-soluble ash-forming elements due to rain. The  
49  
50 barley husk was sourced from the same area, and so were wastes from the milling and refining  
51  
52 process of barley grains. The received fuels were milled in a hammer mill to particles with size <  
53  
54 3 mm. The properties of two fuels are listed in Table 1. The marble sludge was obtained as slurry  
55  
56  
57  
58  
59  
60

1  
2  
3  
4  
5  
6 from the marble processing company Hustadmarmor AS in Fræna, Norway. The received marble  
7  
8 sludge was further air-dried to have a moisture content of ~10%. The calcium lignosulfonate was  
9  
10 dry light-yellow and brown powders from Borregaard ASA. Both marble sludge and calcium  
11  
12 lignosulfonate were further milled and sieved to a particle size < 20 µm.

13  
14  
15  
16 The pellets of barley straw and barley husk with or without additive addition were produced using  
17  
18 a pellets press (Kahl Akamat Herba-A/5K) equipped with a cascade mixer. The barley straw or  
19  
20 barley husk was first milled and then transported to the mixer. For producing additive blended  
21  
22 pellets, the fine additive powders were fed into the cascade mixer constantly through a feeding  
23  
24 tube, which were stirred and blended with fuel particles by mixing paddles. After conditioning, the  
25  
26 materials in the mixer passed through a rotating horizontal die and were pressed into pellets. The  
27  
28 blending ratio of the additive to fuel was controlled by adjusting the mass of the additive fed into  
29  
30 the mixer per unit time. In this way, fuel pellets with or without additive addition were produced  
31  
32 under similar pelletizing conditions. Before pellets production, preliminary experiments were done  
33  
34 for evaluating the effect of an additive on fuel ash melting behavior with respect to different  
35  
36 additive-to-fuel ratios (0-5 wt%). Based on the assessment of ash melting behavior, marble sludge  
37  
38 and calcium additive were added corresponding to approximately 3 wt% of each dry fuel. In  
39  
40 addition, the calcium based additives lime and limestone were investigated as additive to reduce  
41  
42 ash slagging during the combustion of cereal grains rich in phosphorus. It was reported that an  
43  
44 additive-to-fuel ratio of 3 wt% dry substance was sufficient to eliminate slag formation during  
45  
46 wheat grain combustion.<sup>9,24</sup> Therefore, the same additive-to-fuel ratio was also selected and studied  
47  
48 in the present work for comparison purpose. Moreover, addition of 3 wt% dry substance additive  
49  
50 to the fuel pellets only results in a small increase of amount of ingoing ash to the burner, which  
51  
52 does not cause significant ash handling burdens. In this work, fuel pellets were also produced with  
53  
54  
55  
56  
57  
58  
59  
60



1  
2  
3  
4  
5  
6 addition of both 3 wt% marble sludge and 3 wt% calcium additive. The two additives were added  
7  
8 into one fuel to search for possible synergy effects from them on both pellets quality and ash  
9  
10 slagging behaviors. In total, 8 types of pellets were produced for further combustion experiments.  
11  
12

## 13 **2.2 Characterization of Produced Pellets**

14  
15  
16 The properties of barley straw and barley husk pellets with or without additives addition were  
17  
18 further characterized. The melting characteristics of ashes from the produced pellets were  
19  
20 determined by following procedures described in Standard ISO 540: 1995.<sup>27</sup> The ash from each  
21  
22 type of pellet was produced through burning the sample at 550 °C for 12 hours according to ASTM  
23  
24 D 1102.<sup>28</sup> The residue ash was then collected and shaped into a 3 x 3 mm cubical specimen. The  
25  
26 ash specimens were loaded into an analyzer and heated from room temperature to 1500 °C at 6  
27  
28 °C/min in oxidizing atmosphere. Shape changes of each ash specimen were recorded as  
29  
30 temperature increases via a high-speed video camera. According to the standard, four ash fusion  
31  
32 characteristic temperatures were determined based on the shape changes of one sample, i.e. initial  
33  
34 deformation temperature (IDT), softening temperature (ST), hemisphere temperature (HT) and  
35  
36 fluid temperature (FT). Five tests were performed for each ash sample, and the average values are  
37  
38 presented in Table 2.  
39  
40  
41  
42

## 43 **2.3 Combustion Experiments**

44  
45  
46 The combustion of the selected pellets was performed in a 25 kW horizontally-fired step-grate  
47  
48 burner (CN-STOKER, type CN 250) connected to a 25 kW boiler (CN-boiler CN25) at full loads.  
49  
50 The boiler consists of a furnace chamber and a 2-way heat exchanger, with all parts being water  
51  
52 jacketed. Depending on the bulk densities of fuel pellets, a total of 50-60 kg for each fuel was  
53  
54 combusted. Temperatures at different positions in the burner were measured by shielded type K  
55  
56 thermocouples. One thermocouple was mounted approximately 50 mm over the grate for recording  
57  
58  
59  
60

1  
2  
3  
4  
5  
6 combustion temperature. Continuous measurement of O<sub>2</sub>, CO and NO in the flue gas was  
7  
8 conducted online using a flue gas analyzer (TESTO 354/450 XL). After each combustion  
9  
10 experiment, the amounts of ash residues in the burner and boiler were collected and quantified, and  
11  
12 were then analyzed.

#### 13 14 15 16 **2.4 Visual Evaluation and Chemical Characterization of the Collected Ash Samples**

17  
18 The sintering degree of the ash residues was assessed both through visual inspection together with  
19  
20 a simple strength by bare hand. The slag samples were classified according to a scale as follows:

21  
22 (1) non-sintered ash residues, (2) slightly sintered ash with a fragile structure that is easily broken,  
23  
24 (3) very hard sintered ash that fused into small size and breakable slags and (4) completely melted  
25  
26 ash that fused into large blocks and lumps. A similar scale for grading sintering degree of ash has  
27  
28 been used in previous studies focusing on biomass pellets combustion applications.<sup>7-9</sup> The collected  
29  
30 ash residues were further sieved and all melted ash particles larger than 0.3 cm were removed and  
31  
32 classified as slag. The rest of the ash residues after sieving was considered as bottom ash. This  
33  
34 assessment procedure was developed and used in various studies and proven to be an efficient way  
35  
36 for evaluating slagging tendency and degree of different biomass fuels.<sup>8-10, 24</sup>

37  
38  
39  
40  
41  
42 The chemical compositions of the bottom ash and slag were determined by X-ray fluorescence  
43  
44 (XRF). A Bruker D8 Advance X-ray diffractometer using Cu k-alpha radiation and a LynxEye  
45  
46 detector was used for identifying mineral phases in the bottom ash and slag. An instrument  
47  
48 integrated TOPAS evaluation program and the ICDD-PDF2 database were used for processing  
49  
50 obtained X-ray spectra. The morphology and microchemistry of the slag samples were examined  
51  
52 by Scanning Electron Microscopy (SEM) equipped with Energy Dispersive X-ray Fluorescence  
53  
54 spectrometry (EDX). Representative slag samples were mounted in resin, and then cut, ground and  
55  
56 polished to obtain cross-sections with smooth surfaces. Back-scattered electron (BSE) images were  
57  
58  
59  
60

1  
2  
3  
4  
5  
6 taken from scan areas. For the same areas, EDX spot analyses were performed using EDX, and  
7  
8 element maps were also obtained to show the distribution and correlations of important elements  
9  
10 in the sample.

### 11 12 13 **3 RESULTS AND DISCUSSION**

#### 14 15 16 **3.1 Characterization of Fuels, Additives and Produced Pellets**

17  
18 The fuel and additive analysis results are shown in Table 1. The barley straw and barley husk have  
19  
20 high heating values around 19 MJ/kg<sub>d.b.</sub> Compared to conventional woody biomass, the ash content  
21  
22 of the two fuels are rather high. Chemical analysis results showed that barley straw ash, produced  
23  
24 at 550 °C according to standard ASTM D1102 in lab, has similar characteristics as other  
25  
26 agricultural wastes such as rice and wheat straw.<sup>10</sup> Potassium, silicon and calcium are three  
27  
28 dominant elements in the barley straw ash produced at 550 °C, with small contents of phosphorus  
29  
30 and magnesium. The silicon content of the barley straw ash is 10% higher than that of the barley  
31  
32 husk ash. For crop straw, silicon is a key element to form silicate skeleton on the surface of straw  
33  
34 and strengthen the microstructure.<sup>29</sup> In addition, concentration of silicon in crop straw can also be  
35  
36 enhanced due to soil contamination. Different from the barley straw, the barley husk has a  
37  
38 substantially high phosphorous content that is almost three times of that in the barley straw. The  
39  
40 abundance of phosphorous in the seed-originating biomass materials like wheat bran, cereal grain  
41  
42 and meals was reported previously.<sup>8, 13-15</sup> Phosphorus is a vital nutrient for cell division and  
43  
44 development of new tissues, which is essential for seeds formation and growth consequently.<sup>14</sup>  
45  
46 Therefore, a large amount of phosphorous are found in seeds, cereals, grains, husks and grans.<sup>11-13</sup>  
47  
48 Most of the phosphorous in the wheat gran is present as phytic acid or phytate, which convert to  
49  
50 K-phosphates, Mg-phosphates, K-Mg-phosphates or phosphorus oxides.<sup>13, 14, 30</sup> These P-rich fuels  
51  
52 are often related to high ash sintering and slagging tendencies.<sup>8</sup> The calcium lignosulfonate has an  
53  
54  
55  
56  
57  
58  
59  
60

1  
2  
3  
4  
5  
6 ash content of 23.2 wt% on dry substance base, and is dominated by the elements calcium and  
7  
8 sulfur. In addition to ash content, the heating value of the calcium additive is significantly high. It  
9  
10 indicates that the burning of calcium lignosulfonate can also contribute to energy production during  
11  
12 pellets combustion processes. Marble sludge contains calcium as a dominating element, and with  
13  
14 a small amount of magnesium. As showed in Table 2, addition of calcium lignosulfonate improved  
15  
16 the durability of barley straw and husk pellets. The calcium lignosulfonate contains certain amount  
17  
18 of sulfonated random water-soluble polymers. As the calcium lignosulfonate encounters moisture  
19  
20 in the studied biomass fuels, it becomes tacky and makes particles stick together.<sup>31</sup> Therefore, the  
21  
22 lignosulfonate acts as a binder to improve durability and strength of biomass pellets. This will  
23  
24 reduce weight loss related to the formation of fines during pellets transportation and storage.<sup>32</sup> On  
25  
26 the other hand, addition of marble sludge only enhanced the durability of the barley husk pellets.  
27  
28 As an inorganic additive, marble sludge might affect bonding of biomass fuel particles in different  
29  
30 ways, which cause variation in pellets quality consequently. The barley husk ash started to melt at  
31  
32 around 860 °C and completely melted at 1104 °C already. The barley straw ash has significantly  
33  
34 higher ash fusion characteristics temperatures, and melts at about 964 °C and is fully fused at 1186  
35  
36 °C. In addition, for both the barley husk and barley straw, from initial melting to full fusion took a  
37  
38 very short time interval, i.e. occurred in a narrow temperature range, with observation of clear  
39  
40 swelling and bubbling of ash specimens during ash fusion tests. The ash fusion test results indicate  
41  
42 high sintering and slagging tendency of both barley straw and barley husk at elevated temperatures.  
43  
44 Addition of additives significantly increased fusion temperatures of barley straw and barley husk  
45  
46 ashes by 90-200 °C. Addition of both calcium lignosulfonate and marble sludge has distinctive  
47  
48 enhancing effects on the melting temperature of ashes from two fuels.  
49  
50  
51  
52  
53  
54  
55

### 56 57 58 3.2 Combustion Experiments and Slagging Tendency 59 60

1  
2  
3  
4  
5  
6 In all combustion experiments, combustion temperatures in the vicinity of the burner and flue gas  
7  
8 compositions were continuously measured. The maximum temperature measured in the region  
9  
10 above the grate was in the range of 1130 °C and 1180 °C. During combustion of barley straw and  
11  
12 barley husk pellets with additive blended, the measured maximum temperatures only slightly  
13  
14 increased, which should not give significant effects on the slag formation. The O<sub>2</sub> level in the flue  
15  
16 gases was in level 5-7 volume%. The average CO emission levels increased from 20-50 ppm to  
17  
18 117-250 ppm as the barley straw and barley husk pellets with different additives blended were  
19  
20 burned. The measured emission levels of NO<sub>x</sub> were in a range of 370-470 ppm.  
21  
22

23  
24 Each combustion experiment was planned to last 5 hours to produce enough representative ash  
25  
26 samples. However, the combustion of barley straw and barley husk pellets only lasted around 30-  
27  
28 40 minutes from starting the firing to stopping the fuel feeding due to intensive formation of ash  
29  
30 slag. Most formed ash slag piled up on burner grate, causing severe clogging of primary air inlets  
31  
32 and eliminating combustion of incoming fuel pellets consequently. Upon addition of calcium  
33  
34 lignosulfonate, severe ash slagging was evidently reduced during combustion of barley straw and  
35  
36 husk pellets. Only a few large hard slag blocks and many small lumps were formed. Marble sludge  
37  
38 addition eliminated slag formation during the combustion of the two kinds of fuel pellets. The ash  
39  
40 residues left in the burner were powders that traveled along the burner and fell down into the ash  
41  
42 pan. There was also no slag formation during combustion of the barley straw and husk with addition  
43  
44 of both calcium lignosulfonate and marble sludge. The slagging tendency of barley straw and  
45  
46 barley husk pellets with or without additives addition were expressed as fraction of ingoing fuel  
47  
48 ash that formed as slag. As shown in Figure 1, both barley straw and barley husk pellets have high  
49  
50 slagging tendency, with 38% and 56% of ingoing ash forming slag during combustion tests. The  
51  
52  
53  
54  
55  
56  
57  
58  
59  
60  
slag from the combustion of barley straw and barley husk pellets were completely melted, and

1  
2  
3  
4  
5  
6 classified as the highest sintering degree, i.e. a scale of 4. Figure 2 shows representative slag  
7  
8 samples with similar sizes collected after combustion of barley straw and husk pellets with and  
9  
10 without addition of calcium lignosulfonate. Figure 2a shows that the barley straw ash slag has  
11  
12 continuous dense compact structure, which is hard as stone and cannot break with bare hand. On  
13  
14 the other hand, the barley husk slag has a rather porous structure with many openings on the surface  
15  
16 and in fractured areas. It indicates that the barley husk ash passed through a severe molten phase  
17  
18 and acted as liquid with intensive bubbling. The 3% calcium lignosulfonate addition to the pellets  
19  
20 had significant positive effect on the slagging tendency of two studied fuels. As shown in Figure  
21  
22 2, only about 21% and 34% of the ingoing ash formed as slag during combustion of barley straw  
23  
24 and husk with addition of calcium lignosulfonate, respectively. The slag samples from the  
25  
26 combustion of calcium lignosulfonate added pellets have different sintering degrees. The major  
27  
28 fraction of them has low sintering degree, and are breakable structures that can be pressed into  
29  
30 powders by fingers. There is also a minor fraction of slag formed due to sintering and aggregation  
31  
32 of ash, which are rather hard to break into pieces as shown in Figure 2b and 2d.  
33  
34  
35  
36  
37  
38

### 39 3.3 Chemical Composition of Bottom Ash and Slag Formation without Additives

40  
41  
42 The chemical compositions of the formed slag and bottom ash are presented in Figures 3-5. The  
43  
44 dominating elements in the slag from combustion of barley straw pellets are silicon, potassium,  
45  
46 and calcium, indicating that the presence of various silicates. The chemical analyses results showed  
47  
48 that major elements in the barley husk slag are silicon, potassium and phosphorus, with lower  
49  
50 contents of calcium and magnesium as well. The concentration of phosphorus in the barley husk  
51  
52 slag is significantly higher than that of barley straw slag. Additionally, the calcium content in the  
53  
54 barley husk slag is 15% less than that of barley ash slag. Differences in the concentrations of  
55  
56 dominating elements in the slags imply different ash transformation reactions and slag forming  
57  
58  
59  
60

1  
2  
3  
4  
5  
6 mechanisms during combustion of the barley straw and husk pellets. In comparison to the barley  
7  
8 husk, the content of potassium in the barley straw slag and bottom ash are considerably higher.  
9  
10 **Amounts** of silicon and chlorine in the raw biomass, among other factors, is a crucial factor to  
11  
12 determine retention of potassium in the ash residues. During combustion of biomass fuel, chlorine  
13  
14 is a key inorganic element facilitating potassium release that is limited by the quantity of available  
15  
16 chlorine.<sup>33, 34</sup> For chlorine rich biomass fuel, a larger fraction of potassium releases together with  
17  
18 chlorine through sublimation of KCl during the devolatilization of fuel particles <sup>33</sup>. During the char  
19  
20 burnout stage, the residual potassium has great affinity to react with silicon containing species (i.e.,  
21  
22 silica and silicates) to form K-silicates.<sup>5</sup> As seen in Table 1, compared to barley husk, the barley  
23  
24 straw contains evidently higher concentration of silicon and lower concentration of chlorine. This  
25  
26 ash composition favors formation of K-silicates, retaining in the solid combustion residues and  
27  
28 which partially explain the higher potassium content in the barley straw ash slag and bottom ash  
29  
30 (see Figures 3 and 4). This finding agrees well with that potassium is readily retained in silicon  
31  
32 rich straw ash and slag as reported in previous studies.<sup>5, 29</sup>  
33  
34  
35  
36  
37

38  
39 **Figures 3 and 4 show that the addition of calcium lignosulfonate resulted in a distinct increase of**  
40  
41 **calcium concentration in both slags and bottom ashes formed during combustion of barley straw.**  
42  
43 **Enrichment of calcium is evident for the slag collected from combustion of barley straw, which**  
44  
45 **increased from 22% to 35% upon calcium lignosulfonate addition. On the other hand, the**  
46  
47 **concentration of potassium in slag from the combustion of calcium lignosulfonate added barley**  
48  
49 **straw pellets are evidently lower than that from the combustion of non-additive pellets (see Figure**  
50  
51 **3). Upon addition of calcium lignosulfonate, a great amount of calcium is introduced to barley**  
52  
53 **straw ash. Enhancement of calcium will limit incorporation of potassium into the silicates structure,**  
54  
55 **which releases to gas phase instead.**<sup>30</sup> In addition, it was also reported that calcium, either inherent  
56  
57  
58  
59  
60

1  
2  
3  
4  
5  
6 or from an external source, might substitute K in the molten depolymerized K-silicates to promote  
7 release of K during biomass combustion.<sup>9, 10, 13, 35</sup> Therefore, addition of calcium lignosulfonate  
8 reduces retention of the potassium in the ash and formation of low temperature melting K-silicates  
9 consequently. This is accompanied with decrease in ash melts formed and hence slagging tendency,  
10 as observed in this work. As displayed in Figures 3 and 5, phosphorus is enriched in both slag and  
11 bottom ash upon combustion of barley husk with addition of calcium lignosulfonate. Release of  
12 phosphorus is presumably related to formation and volatilization of K-phosphates (i.e.,  $KPO_3$ )  
13 during combustion of phosphorus rich biomass fuels, which normally end up as fine particles in  
14 the flue gas.<sup>9, 14</sup> In presence of alkali earth metals, chemical transformation reactions of phosphorus  
15 is rather different and more solid ternary phosphates are preferably formed hence remain in ash  
16 residues.<sup>5</sup> Addition of calcium lignosulfonate introduces additional calcium to the barley husk ash  
17 that reduce the extent of phosphorus volatilization and promotes formation of nonvolatile K-Ca-  
18 phosphates. It partially explains enrichment of the phosphorus in the slag and bottom ash from  
19 combustion of calcium lignosulfonate added barley husk pellets. It is worth to note that, upon  
20 addition of calcium lignosulfonate, the contents of sulphur in all analyzed slag and bottom ash  
21 samples are increased considerably. The sulfur should be initially from the calcium additive, and  
22 might also be involved in ash transformation reactions during the combustion of the studied fuel  
23 pellets. As expected, the addition of marble sludge alone or together with calcium lignosulfonate  
24 increased the content of calcium in the barley straw bottom ash dramatically. On the other hand,  
25 the concentrations of silicon and potassium decrease evidently.

26  
27  
28  
29  
30  
31  
32  
33  
34  
35  
36  
37  
38  
39  
40  
41  
42  
43  
44  
45  
46  
47  
48  
49  
50  
51  
52  
53 The crystalline phases in the collected slag and bottom ash samples were further identified by XRD  
54 and the result is listed in Table 3. One should note that the slag and bottom ash contain materials  
55 that are in crystalline or amorphous phases, and the later one cannot be directly observed by XRD.  
56  
57  
58  
59  
60



1  
2  
3  
4  
5  
6 The ratio between crystalline and amorphous phases is strongly affected by fuel chemical  
7 composition, thermal conversion temperatures and ash cooling history etc.  
8  
9

10  
11 As listed in Table 3, only three crystalline phases  $\text{SiO}_2$ ,  $\text{K}_2\text{CaP}_2\text{O}_7$  and  $\text{KMgPO}_4$  are identified in  
12 the barley straw slag. During combustion of biomass, potassium may involve in the formation of  
13 both phosphates and silicates but the phosphorus has a higher thermodynamic affinity than silicon  
14 to react with potassium and that the K-phosphates may form prior to the K-silicates.<sup>5</sup> As the initially  
15 formed K-phosphates encounter the alkali earth metals, ternary K-Ca/Mg-phosphates are readily  
16 formed and remain in the ash residues. Similar observations of  $\text{K}_2\text{CaP}_2\text{O}_7$  and  $\text{KMgPO}_4$  can be  
17 made in the barley straw slag in this study. Formation of K phosphates and K-Ca/Mg-phosphates  
18 reduces the amount of potassium available to react with silicon during combustion of biomass. As  
19 seen for the ash composition (Table 1) of the barley straw, the content of phosphorus and the molar  
20 ratio of Si/K are both rather high. The results suggest that a certain portion of the silicon in the  
21 barley straw, either organically bound or from external sources, keeps unreacted and ends up in the  
22 ash residues as silica. This is consistent with the observation of  $\text{SiO}_2$  as a main crystalline phase in  
23 the slag.  
24  
25  
26  
27  
28  
29  
30  
31  
32  
33  
34  
35  
36  
37  
38  
39

40  
41 Compared to barley straw slag, more K-Ca/Mg-phosphates were identified as major crystalline  
42 phases in the barley husk slag as shown in Table 3. This is related to high content of P in the barley  
43 husk, which favors formation of K-Ca/Mg-phosphates. Again, the  $\text{SiO}_2$  was identified as the other  
44 major crystalline phase in the barley husk ash. Similar crystalline phases have been identified in  
45 the slag from combustion of phosphorus rich barley grains.<sup>8</sup> The results reported in this study,  
46 together with those in in previous work <sup>11</sup>, confirm that different ash transformation chemical  
47 reactions during the combustion of phosphorus-rich and -poor biomass fuels have important effect  
48 on the mechanisms and severity of ash slagging.  
49  
50  
51  
52  
53  
54  
55  
56  
57  
58  
59  
60

1  
2  
3  
4  
5  
6 As seen in Table 3, compared to slag formed from the combustion of pellets without additives,  
7  
8 there are evident differences of mineralogical phases identified from the slags collected after  
9  
10 combustion of barley straw and barley husk pellets with addition of additives. Upon addition of  
11  
12 calcium lignosulfonate, new mineral phases  $\text{Ca}_2\text{SiO}_4$  and  $\text{Ca}_2\text{Mg}(\text{Si}_2\text{O}_7)$  were observed from the  
13  
14 barley straw slag, with no crystallized  $\text{SiO}_2$  detected in the same sample. For the agricultural wastes  
15  
16 such as crop straws, silicon and potassium in the fuel are abundantly available and readily react  
17  
18 during combustion. Products from such reactions are normally K-silicates that readily melt,  
19  
20 initiating and enhancing ash sintering and slagging. As the molten K-silicates encounter the alkali  
21  
22 earth metal oxides, reactions will take place and the latter will dissolve into the melts, resulting in  
23  
24 evaporation of K and formation of Ca/Mg-silicates and/or K-Ca/Mg-silicates. The formed Ca/Mg-  
25  
26 silicates and/or K-Ca/Mg-silicates normally have much high melting temperature compared to the  
27  
28 initially formed K-silicates.<sup>8</sup> Formation of these melting phases of high melting points resulted in  
29  
30 reduction of ash melts amount in the slag and slag sintering degree as well. The other possible  
31  
32 explanation for this is that calcium oxide contained in the calcium lignosulfonate might directly  
33  
34 react with the silica in the barley straw ash, leading to the formation of  $\text{Ca}_2\text{SiO}_4$  and  $\text{Ca}_2\text{Mg}(\text{Si}_2\text{O}_7)$   
35  
36 both of which have high melting points and are thermally stable. Since silica in the barley straw  
37  
38 can react with calcium oxide from the additive, less amounts of silica in fuel will be available to  
39  
40 form molten K-silicates that are key sources for producing ash melts. It explains decreased slag  
41  
42 sintering degrees during barley straw combustion with addition of the calcium additive.  
43  
44  
45  
46  
47  
48  
49

50  
51 As can be observed in Table 3, the addition of calcium additive resulted in a general shift from  
52  
53 potassium rich phosphates (i.e.,  $\text{K}_2\text{Ca}_2\text{P}_2\text{O}_7$ ) to calcium rich phosphates [i.e.,  $\text{Ca}_{10}\text{K}(\text{PO}_4)_7$  and  
54  
55  $\text{KCaPO}_4$ ] in the slags from the combustion of barley husk pellets. As aforementioned, intensive  
56  
57 formation of potassium phosphates may take place during the combustion of the barley husk  
58  
59  
60

1  
2  
3  
4  
5  
6 pellets, considering the high contents of both phosphorus and potassium in the fuel. The addition  
7  
8 of calcium lignosulfonate provides calcium oxide to react with K-phosphates formed initially to  
9  
10 produce Ca rich K-Ca-phosphates. The latter ones normally have higher melting points and can  
11  
12 explain the improved slagging behavior of the barley husk ash. Similar ash transformation  
13  
14 chemistry was also observed during the combustion of phosphorus rich cereal grains with addition  
15  
16 of 2 wt% of lime.<sup>8</sup> In addition to K-Ca-phosphates, a small amount of  $\text{Ca}_2\text{Mg}(\text{Si}_2\text{O}_7)$  was also  
17  
18 observed from slag collected from the combustion of barley husk pellets with addition of calcium  
19  
20 lignosulfonate. The results suggest that a redistribution of Si from potassium silicates to calcium  
21  
22 silicates that have high melting points. This might also contribute to the reduction in the amount  
23  
24 and sintering degree of ash slag formed during the combustion of the barley husk pellets with prior  
25  
26 blending of the calcium additive.  
27  
28  
29  
30  
31

32 Table 3 also lists the crystalline phases observed from the bottom ash samples. In addition to the  
33  
34 K-Ca-phosphates and  $\text{SiO}_2$ , there are also crystalline phases KCl and  $\text{K}_2\text{SO}_4$  detected from bottom  
35  
36 ashes from the combustion of barley straw and husk pellets. These two major crystalline phases  
37  
38 are presumably formed and vaporized during initial combustion of the biomass fuel pellets  
39  
40 produced from agricultural and food processing wastes.<sup>10</sup> During the shutdown and cooling stages  
41  
42 of the combustion experiments, these phases may be crystallized out from the flue gas and  
43  
44 condensed on the surfaces of bottom ash particles.<sup>8</sup> It should be noted that the amount of  $\text{K}_2\text{SO}_4$  in  
45  
46 the bottom ashes increased during combustion after the addition of calcium lignosulfonate into the  
47  
48 barley straw and husk pellets. While the exact mechanism is unknown, one possible interpretation  
49  
50 is that the calcium lignosulfonate contains a high content of sulfur that will be oxidized first and  
51  
52 then react with potassium in the fuel pellets during the combustion tests. This leads to a subsequent  
53  
54 increase of the  $\text{K}_2\text{SO}_4(\text{g})$  concentration in the flue gas, which condense on bottom ash particle  
55  
56  
57  
58  
59  
60

1  
2  
3  
4  
5  
6 surfaces, as detected by XRD. Compared to those from the combustion of pellets without additives,  
7  
8 significant amounts of  $\text{CaCO}_3$  and  $\text{CaO}$  were identified in the bottom ash samples from pellets  
9  
10 combustion with the addition of either calcium lignosulfonate or marble sludge. This is more  
11  
12 evident for the bottom ashes from the combustion of marble sludge blended pellets. The presence  
13  
14 of  $\text{CaCO}_3$  and  $\text{CaO}$  indicates there is surplus marble sludge in the system. Therefore, a dilution  
15  
16 effect from the marble sludge on the barley straw and husk ash during combustion should be taken  
17  
18 into account regarding slag formation. In addition,  $\text{Ca}_5(\text{PO}_4)_3(\text{OH})$  was also observed from the  
19  
20 bottom ash samples collected from combustion of fuel pellets with marble sludge blended.  
21  
22 Formation of  $\text{Ca}_5(\text{PO}_4)_3(\text{OH})$  is probably due to reactions between calcium rich phosphates and  
23  
24 water vapors from fuel pellets.<sup>8</sup> Similar phase compositions have been observed in bottom ashes  
25  
26 from combustion of cereal crops with addition of lime.<sup>8</sup>  
27  
28  
29  
30  
31

### 3.4 SEM-EDX analysis of slag

32  
33  
34  
35 Figure 6 shows the representative back-scattered electron images of cross-sections of slag samples  
36  
37 collected from combustion of barley straw and barley husk with and without addition of calcium  
38  
39 lignosulfonate. It can be seen that both barley straw and husk slag have a continuous and dense  
40  
41 structure with inclusion of many voids with round rims (see panels a and b of Figure 6). The round  
42  
43 voids represent formation of bubbles due to release of gases from the barley straw and husk ash  
44  
45 that melted severely in a liquid phase with high surface tensions. The slag samples formed upon  
46  
47 addition of calcium lignosulfonate (see panels c and d of Figure 6) have rather heterogeneous  
48  
49 structure with reduced number of round voids. There are also areas and patches with higher  
50  
51 brightness, which are absent in the BSE images of slag from combustion of non-additive pellets. It  
52  
53 indicates that different compositional phases exist in slag formed with or without additive addition.  
54  
55  
56  
57  
58  
59  
60

1  
2  
3  
4  
5  
6 Figure 7 shows a BSE image of a scanned area (100 x 100  $\mu\text{m}$ ) of cross-sectioned barley straw ash  
7 slag. Three zones can easily be distinguished according to brightness. The zone with dark gray  
8 color dominates the whole scanned area. EDX spot analyses (spots 1 and 2, Figure 8) revealed that  
9 potassium and silicon are two main elements, with clear correlations in the elemental maps (Figure  
10 7). It manifests that slag from barley straw combustion contains melted potassium silicates. This  
11 finding agrees well with the previous work.<sup>10, 29</sup> It was reported that the potassium silicates  
12 chemistry plays a critical role in ash slagging during the combustion of silicon rich agricultural  
13 residues.<sup>10, 29</sup> The zones with light gray color (spots 3 and 4, Figure 8) with round edge can easily  
14 be distinguished in the elemental maps. High contents of potassium and phosphorus and minor  
15 amounts of calcium were detected in these zones, representing the formation potassium-rich  
16 phosphates in the slag. The dark gray zone represents a sand particle trapped by the melted ash, in  
17 which silicon is detected as the main element (spot 5, Figure 8). For the barley straw slag,  
18 significantly high contents of silicon and potassium were detected by both XRF and SEM-EDX  
19 analyses. However, only the  $\text{SiO}_2$ ,  $\text{K}_2\text{CaP}_2\text{O}_7$  and  $\text{KMgPO}_4$  are mineral phases containing silicon  
20 and potassium, as detected by XRD. There is evident deficiency of silicon and potassium detected  
21 in the XRD analysis compared to those detected by XRF and SEM-EDX analyses. Together with  
22 the clear correlation between silicon and potassium shown in Figure 7, the barley straw slag  
23 presumably contains considerable amount K-silicates that are in glass phases and which cannot be  
24 directly observed by XRD. Actually, for all XRD patterns obtained from the analyzed samples, the  
25 typical scattering distribution from an amorphous material was observed, implying presence of a  
26 significant amount of glass phase.

27  
28  
29  
30  
31  
32  
33  
34  
35  
36  
37  
38  
39  
40  
41  
42  
43  
44  
45  
46  
47  
48  
49  
50  
51  
52  
53  
54  
55 Figure 9 shows BSE image and element mapping of a scanned area (100 x 100  $\mu\text{m}$ ) of barley husk  
56 slag. From the dominating dark gray color zone (spot 1 and 2, Figure 10), silicon, potassium and  
57  
58  
59  
60

1  
2  
3  
4  
5  
6 phosphorus were detected as major elements and the phosphorus content is considerably higher  
7  
8 than that of barley straw slag. It indicates coexistence of potassium-rich silicates and phosphates  
9  
10 in the examined area. It was suggested that phosphates are miscible with silicate melts, leading to  
11  
12 formation of a complex mixture containing both phosphates and silicates.<sup>22, 36</sup> The formed  
13  
14 phosphate-silicate mixture has even lower eutectic points than the parental silicates and  
15  
16 phosphates.<sup>22</sup> Therefore, the formation and melting of a phosphate-silicate mixture could be one  
17  
18 reason for the severe slagging of the barley husk ash observed in this study. There are also some  
19  
20 zones (spots 4-7, Figure 9) with irregular shapes showing in the Figure 9. Potassium, phosphorus,  
21  
22 calcium and magnesium were detected as dominating elements that show clear correlations in  
23  
24 element maps. Therefore, these zones indicate the presence of K-Ca/Mg-phosphates that agree with  
25  
26 XRD analysis results. An extremely high silicon concentration was detected from one of the dark  
27  
28 zones (spot 3, Figure 9), which was easily distinguished due to its high brightness in the right corner  
29  
30 of the elemental Si map (Figure 11). Therefore, this zone represents sand/soil particles trapped in  
31  
32 the melted ash. The SiO<sub>2</sub> is the main mineral composition of these sand/soil particles. The  
33  
34 observation from these sand/soil particles might correlate with identification of SiO<sub>2</sub> in the slag  
35  
36 sample by XRD analysis.  
37  
38  
39  
40  
41  
42

43 Figures 11 and 12 present SEM-EDX analyses of the slag formed during the combustion of barley  
44  
45 straw with addition of calcium lignosulfonate. The results showed that, compared to slag from  
46  
47 barley straw combustion (Figure 8), the slag from the combustion of barley straw with addition of  
48  
49 calcium lignosulfonate (Figure 12) has considerably higher calcium content and lower potassium  
50  
51 content. The EDX analyses results agree well with the bulk chemical composition analysis (XRF)  
52  
53 results shown in Figure 3. The differences in potassium and calcium content shown in Figures 3, 8  
54  
55 and 9 imply reactions between calcium from calcium lignosulfonate and the molten K-silicates in  
56  
57  
58  
59  
60

1  
2  
3  
4  
5  
6 barley straw ash, which enhances potassium release consequently. As shown in the BSE image in  
7  
8 Figure 11, there are many light gray patches distributed across the scanned area. The calcium was  
9  
10 detected as a dominant element (more than 50 %) together with potassium and silicon (spots 3 and  
11  
12 4, Figure 12) and there are clear correlations between the three elements shown in the elemental  
13  
14 maps. Therefore, these light gray patches represent the formation of calcium rich silicates in the  
15  
16 barley straw ash upon addition of calcium lignosulfonate. Figures 13-14 present SEM-EDX  
17  
18 analysis of the slag formed during the combustion of calcium lignosulfonate blended barley husk  
19  
20 pellets. Large amounts of light gray patches and areas are clearly shown in the BSE image in Figure  
21  
22 13, which cannot be found from that of barley husk slag (Figure 9). A significantly high content of  
23  
24 calcium was detected in these patches with relatively small amounts of potassium and phosphorus  
25  
26 (spots 5-9, Figure 14). With addition of calcium lignosulfonate, more calcium is available for  
27  
28 incorporation into K rich phosphates during combustion of barley husk, yielding calcium rich  
29  
30 phosphate with high melting temperatures, as identified by XRD. Considering this, these patches  
31  
32 represent the existence of calcium rich phosphates in the slag.  
33  
34  
35  
36  
37  
38  
39

#### 40 **4 CONCLUSIONS**

41  
42  
43 The study results showed high slagging tendency during combustion of barley straw and barley  
44  
45 husk pellets. The barley straw slag consisted of mainly potassium rich silicates and high  
46  
47 temperature melting potassium calcium phosphates. SiO<sub>2</sub> was also identified from the slag sample.  
48  
49 For barley husk, the collected slag presumably consists of a mixture of potassium rich silicates and  
50  
51 phosphates. Addition of marble sludge or a mixture of it with calcium lignosulfonate eliminated  
52  
53 slag formation during combustion of barley straw and husk pellets. Upon marble sludge addition,  
54  
55 the main composition of the barley straw and husk slag and bottom ash shifted from low melting  
56  
57  
58  
59  
60

1  
2  
3  
4  
5  
6 points silicates and phosphates to high temperature melting calcium silicates, phosphates and  
7  
8 oxides. The significant amount of calcium oxide and calcite carbonate observed in the ash residues,  
9  
10 indicates a surplus of marble sludge that gave a diluting effect and presumably restrains ash  
11  
12 slagging. Addition of calcium lignosulfonate gave a less pronounced effect on mitigation of barley  
13  
14 straw and husk ash slagging. However, as a result of the addition of calcium additive, the slagging  
15  
16 tendencies of the two studied fuels were reduced to certain extents. The size and sintering degree  
17  
18 of the formed slag were considerably decreased. Addition of calcium additive promoted formation  
19  
20 of high temperature melting calcium rich silicates and phosphates in barley straw and husk pellets  
21  
22 ash, respectively. The effect of calcium lignosulfonate addition on barley straw and husk pellets  
23  
24 ash transformation is supported by coherence between the SEM-EDX, XRF and XRD analyses.  
25  
26  
27  
28  
29  
30  
31

## 32 **ACKNOWLEDGMENT**

33  
34 Financial support from the Research Council of Norway through the Bioenergy Innovation Centre  
35  
36 (CenBio) and project GrateCFD is gratefully acknowledged. The authors are grateful to Børre  
37  
38 Heggenhaugen at Nes Forforedling AS for manufacturing pellets. The research also received partial  
39  
40 support from the Australian Research Council via the Discovery Projects scheme.  
41  
42  
43  
44  
45  
46  
47  
48  
49  
50  
51  
52  
53  
54  
55  
56  
57  
58  
59  
60



## REFERENCES

1. Wang, L.; Skreiberg, Ø.; Becidan, M.; Li, H., *Applied Energy* **2016**, 162, 1195-1204.
2. Wang, L.; Becidan, M.; Skreiberg, Ø., *Energy & Fuels* **2012**, 26, (9), 5917-5929.
3. Chen, W.-H.; Peng, J.; Bi, X. T., *Renewable and Sustainable Energy Reviews* **2015**, 44, 847-866.
4. Näzelius, I.-L.; Fagerström, J.; Boman, C.; Boström, D.; Öhman, M., *Energy & Fuels* **2015**, 29, (2), 894-908.
5. Boström, D.; Skoglund, N.; Grimm, A.; Boman, C.; Öhman, M.; Broström, M.; Backman, R., *Energy & Fuels* **2011**, 26, (1), 85-93.
6. Wang, L.; Skjevrak, G.; Hustad, J. E.; Skreiberg, Ø., *Energy & Fuels* **2014**, 28, (1), 208-218.
7. Öhman, M.; Boström, D.; Nordin, A.; Hedman, H., *Energy & Fuels* **2004**, 18, (5), 1370-1376.
8. Lindström, E.; Sandström, M.; Boström, D.; Öhman, M., *Energy & Fuels* **2007**, 21, (2), 710-717.
9. Boström, D.; Grimm, A.; Boman, C.; Björnbom, E.; Öhman, M., *Energy & Fuels* **2009**, 23, (10), 5184-5190.
10. Gilbe, C.; Öhman, M.; Lindström, E.; Boström, D.; Backman, R.; Samuelsson, R.; Burvall, J., *Energy & Fuels* **2008**, 22, (5), 3536-3543.
11. Lindström, E.; Larsson, S. H.; Boström, D.; Öhman, M., *Energy & Fuels* **2010**, 24, (6), 3456-3461.
12. Magdziarz, A.; Gajek, M.; Nowak-Woźny, D.; Wilk, M., *Renewable Energy* **2017**.
13. Steenari, B. M.; Lundberg, A.; Pettersson, H.; Wilewska-Bien, M.; Andersson, D., *Energy & Fuels* **2009**, 23, 5655-5662.
14. Wu, H.; Castro, M.; Jensen, P. A.; Frandsen, F. J.; Glarborg, P.; Dam-Johansen, K.; Røkke, M.; Lundtorp, K., *Energy and Fuels* **2011**, 25, (7), 2874-2886.
15. Piotrowska, P.; Grimm, A.; Skoglund, N.; Boman, C.; Öhman, M.; Zevenhoven, M.; Boström, D.; Hupa, M., *Energy & Fuels* **2012**, 26, (4), 2028-2037.
16. Wang, L.; Skjevrak, G.; Hustad, J. E.; Grønli, M.; Skreiberg, Ø. In *Effects of additives on barley straw and husk ashes sintering characteristics*, Energy Procedia, 2012; 2012; pp 30-39.
17. Zevenhoven, M.; Yrjas, P.; Skrifvars, B. J.; Hupa, M., *Energy and Fuels* **2012**, 26, (10), 6366-6386.
18. Niu, Y.; Tan, H.; Wang, X.; Liu, Z.; Liu, H.; Liu, Y.; Xu, T., *Bioresource Technology* **2010**, 101, (23), 9373-9381.
19. Hupa, M.; Karlström, O.; Vainio, E., *Proceedings of the Combustion Institute* **2016**.
20. Hupa, M., *Energy and Fuels* **2012**, 26, (1), 4-14.
21. Pettersson, A.; Zevenhoven, M.; Steenari, B. M.; Åmand, L. E., *Fuel* **2008**, 87, (15-16), 3183-3193.
22. Lindberg, D.; Backman, R.; Chartrand, P.; Hupa, M., *Fuel Processing Technology* **2013**, 105, 129-141.
23. Wang, L.; Hustad, J. E.; Skreiberg, Ø.; Skjevrak, G.; Grønli, M. In *A critical review on additives to reduce ash related operation problems in biomass combustion applications*, Energy Procedia, 2012; 2012; pp 20-29.
24. Xiong, S.; Burvall, J.; Örberg, H.; Kalen, G.; Thyrel, M.; Öhman, M.; Boström, D., *Energy & Fuels* **2008**, 22, (5), 3465-3470.

- 1  
2  
3  
4  
5  
6 25. Wang, L.; Skjevrak, G.; Hustad, J. E.; Grønli, M. G., *Energy & Fuels* **2011**, 25, (12),  
7 5775-5785.  
8 26. Wang, L.; Skreiberg, Ø.; Becidan, M., *Applied Thermal Engineering* **2014**, 70, (2), 1262-  
9 1269.  
10 27. ISO, 540:1995 Solid mineral fuels -Determination of fusibility of ash -- High-temperature  
11 tube method. In 1995.  
12 28. ASTM, D1102 -84(2013) Standard Test Method for Ash in Wood. . In 2013.  
13 29. Knudsen, J. N.; Jensen, P. A.; Dam-Johansen, K., *Energy & Fuels* **2004**, 18, (5), 1385-  
14 1399.  
15 30. Novaković, A.; van Lith, S. C.; Frandsen, F. J.; Jensen, P. A.; Holgersen, L. B., *Energy &*  
16 *Fuels* **2009**, 23, (7), 3423-3428.  
17 31. Hu, Q.; Shao, J.; Yang, H.; Yao, D.; Wang, X.; Chen, H., *Applied Energy* **2015**, 157, 508-  
18 516.  
19 32. Berghel, J.; Frodeson, S.; Granström, K.; Renström, R.; Ståhl, M.; Nordgren, D.; Tomani,  
20 P., *Fuel Processing Technology* **2013**, 112, (Supplement C), 64-69.  
21 33. Johansen, J. M.; Aho, M.; Paakkinen, K.; Taipale, R.; Egsgaard, H.; Jakobsen, J. G.;  
22 Frandsen, F. J.; Glarborg, P., *Proceedings of the Combustion Institute* **2013**, 34, (2), 2363-2372.  
23 34. Wang, L.; Moilanen, A.; Lehtinen, J.; Konttinen, J.; Matas, B. G., *Energy Procedia* **2017**,  
24 105, 1295-1301.  
25 35. Thy, P.; Jenkins, B. M.; Leshner, C. E., *Energy & Fuels* **1999**, 13, (4), 839-850.  
26 36. Skoglund, N.; Grimm, A.; Öhman, M.; Boström, D., *Energy & Fuels* **2014**, 28, (2), 1183-  
27 1190.  
28  
29  
30  
31  
32  
33  
34  
35  
36  
37  
38  
39  
40  
41  
42  
43  
44  
45  
46  
47  
48  
49  
50  
51  
52  
53  
54  
55  
56  
57  
58  
59  
60

1  
2  
3  
4  
5  
6 **Tables and Figures**  
7

8 Table 1. Proximate, Ultimate and Ash Composition of Fuels and Additives  
9

|   | barley<br>straw | barley husk | calcium<br>lignosulfonate | marble<br>sludge |
|---|-----------------|-------------|---------------------------|------------------|
| Proximate analysis (wt %, d.b. <sup>a</sup> ) |                 |             |                           |                  |
| Volatiles matter                              | 79.2            | 81.5        | 57.6                      | nd <sup>c</sup>  |
| Fixed carbon <sup>a</sup>                     | 17.6            | 14.4        | 20.2                      | nd <sup>c</sup>  |
| Ash content                                   | 3.2             | 4.1         | 22.2                      | 98.0             |
| Ultimate analysis (wt %, d.b.)                |                 |             |                           |                  |
| C   | 48.4            | 46.4        | 42.5                      | nd <sup>c</sup>  |
| H   | 5.8             | 6.0         | 4.5                       | nd <sup>c</sup>  |
| N   | 0.72            | 2.0         | 0.13                      | nd <sup>c</sup>  |
| S   | 0.08            | 0.14        | 6.46                      | nd <sup>c</sup>  |
| O <sup>b</sup>                                | 45.0            | 45.46       | 46.41                     | nd <sup>c</sup>  |
| High Heating value (MJ/Kg d.b.)               | 19.36           | 18.92       | 15.42                     | nd <sup>c</sup>  |
| Ash forming elements (wt %) <sup>d</sup>      |                 |             |                           |                  |
| CaO   | 13.43           | 6.89        | 65.32                     | 95.12            |
| SiO <sub>2</sub>                              | 41.50           | 30.95       | 0.12                      | 0.20             |
| K <sub>2</sub> O                              | 29.22           | 32.13       | 0.99                      | 0.02             |
| P <sub>2</sub> O <sub>5</sub>                 | 8.07            | 23.76       | 0.51                      | 0.02             |
| MgO   | 1.91            | 0.15        | 0.01                      | 2.99             |
| SO <sub>3</sub>                               | 3.90            | 1.97        | 32.78                     | 0.05             |
| Al <sub>2</sub> O <sub>3</sub>                | 0.18            | 1.43        | 0.03                      | 0.80             |
| Na <sub>2</sub> O                             | 0.38            | 0.01        | 0.07                      | 0.22             |
| Fe <sub>2</sub> O <sub>3</sub>                | 0.43            | 0.65        | 0.12                      | 0.52             |
| Cl  | 0.98            | 2.06        | 0.05                      | nd <sup>c</sup>  |

10  
11  
12  
13  
14  
15  
16  
17  
18  
19  
20  
21  
22  
23  
24  
25  
26  
27  
28  
29  
30  
31  
32  
33  
34  
35  
36  
37  
38  
39  
40  
41 <sup>a</sup> dry basis; <sup>b</sup> by difference; <sup>c</sup> not detected; <sup>d</sup> the values are in weight percentage of dry ashes  
42 produced at 550 °C.  
43  
44  
45  
46  
47  
48  
49  
50  
51  
52  
53  
54  
55  
56  
57  
58  
59  
60

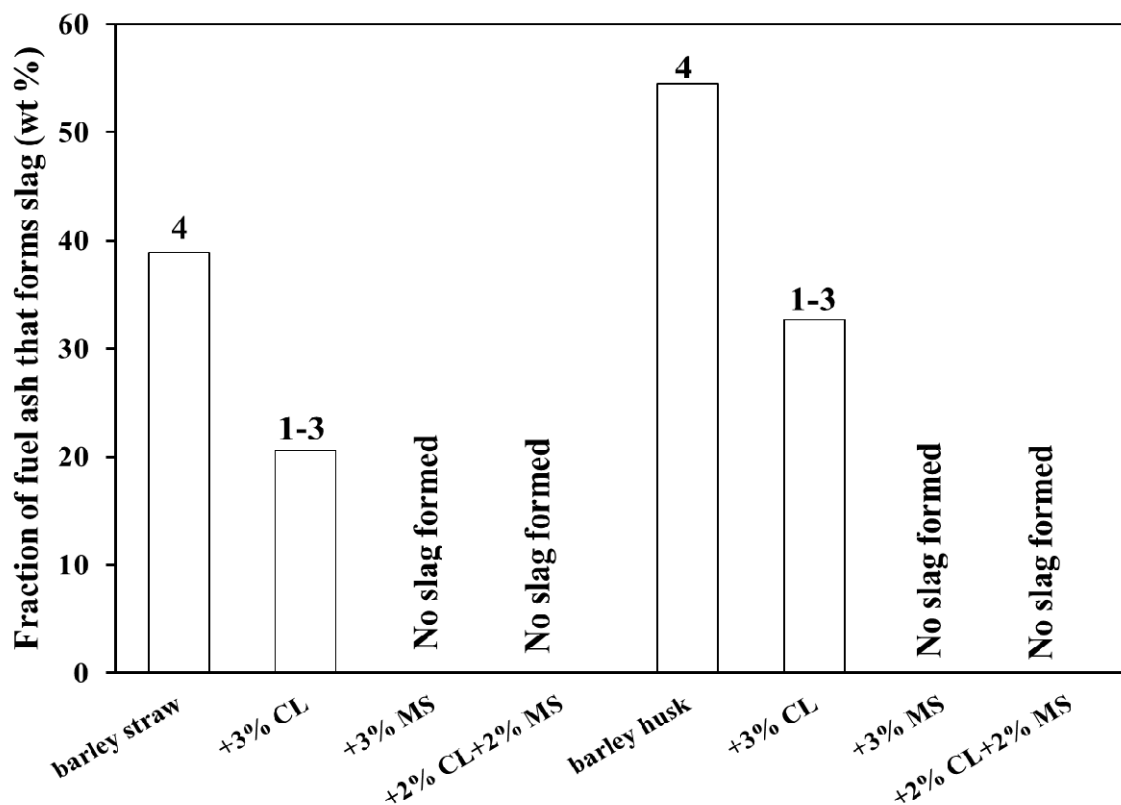
Table 2. Physical Properties and Ash Fusion Behavior of Fuels and Additives

|   | Standard               | barley<br>straw | + 3% CL | +3%<br>MS | + 2% CL<br>+ 2% MS | barley<br>husk | + 3% CL | + 3% MS | + 2% CL +<br>2% MS |
|---|------------------------|-----------------|---------|-----------|--------------------|----------------|---------|---------|--------------------|
| Physical properties of produced fuel pellets  |                        |                 |         |           |                    |                |         |         |                    |
| Particle density (kg/m <sup>3</sup> )   | CEN/TS<br>15405:2006   | 1.25            | 1.23    | 1.29      | 1.32               | 1.24           | 1.25    | 1.27    | 1.28               |
| Bulk density (kg/m <sup>3</sup> )   | NS-EN 15103            | 0.67            | 0.64    | 0.69      | 0.71               | 0.68           | 0.69    | 0.70    | 0.68               |
| Durability (%)  | NS-EN 15210-<br>1:2009 | 95.91           | 98.7    | 90.08     | 94.64              | 88.07          | 93.43   | 93.26   | 94.28              |
| Moisture (wt %)   | NS-EN 14774-2          | 8.42            | 9.96    | 6.59      | 7.03               | 10.98          | 10.65   | 9.88    | 9.98               |
| Ash fusion behavior of pelletized barley straw and husk with and without additives <sup>a</sup> |                        |                 |         |           |                    |                |         |         |                    |
| Initial deformation<br>temperature, IT (°C)   | ISO 540: 1995          | 964             | 1058    | 1108      | 1189               | 860            | 980     | 1022    | 1058               |
| Softening temperature,<br>ST (°C)   | ISO 540: 1995          | 1014            | 1102    | 1208      | 1289               | 972            | 1068    | 1148    | 1204               |
| Hemispherical<br>temperature, HT (°C)   | ISO 540: 1995          | 1098            | 1188    | 1302      | 1346               | 1050           | 1098    | 1264    | 1342               |
| Fluid temperature, FT<br>(°C)   | ISO 540: 1995          | 1186            | 1258    | 1378      | 1388               | 1104           | 1128    | 1348    | 1386               |

<sup>a</sup> the ash was produced at 550 °C according to ASTM Standard D1102.

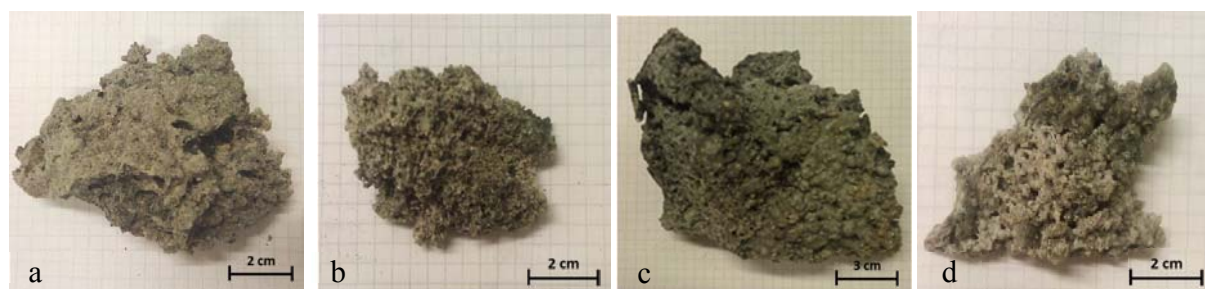
Table 3. XRD analysis on collected slag and bottom ash samples

|  | Slag            |            |                |            | Bottom ash      |            |            |                    |                |            |            |                    |
|--|-----------------|------------|----------------|------------|-----------------|------------|------------|--------------------|----------------|------------|------------|--------------------|
|  | barley<br>straw | + 3%<br>CL | barley<br>husk | + 3%<br>CL | barley<br>straw | + 3%<br>CL | + 3%<br>MS | + 2% CL<br>+ 2% MS | barley<br>husk | + 3%<br>CL | + 3%<br>MS | + 2% CL<br>+ 2% MS |
| SiO <sub>2</sub>   | **              |            | **             |            | **              |            |            |                    | **             |            |            |                    |
| CaK <sub>2</sub> P <sub>2</sub> O <sub>7</sub>                 | **              |            | **             |            | **              |            |            |                    | ***            |            |            |                    |
| Ca <sub>5</sub> (PO <sub>4</sub> ) <sub>3</sub> (O             |                 |            |                |            |                 | **         | **         | **                 |                |            | **         | **                 |
| Ca <sub>10</sub> K(PO <sub>4</sub> ) <sub>7</sub>              |                 |            |                | **         |                 |            |            |                    | *              | **         | **         |                    |
| KMgPO <sub>4</sub>   | *               |            | **             | **         |                 |            |            |                    |                |            |            |                    |
| KCaPO <sub>4</sub>   |                 | **         | **             | ***        |                 |            |            |                    |                |            |            |                    |
| Ca <sub>2</sub> SiO <sub>4</sub>                               |                 | ***        |                |            |                 |            |            |                    |                |            |            |                    |
| CaCO <sub>3</sub>  |                 |            |                |            | *               | ***        | ***        |                    | **             | ***        | ***        |                    |
| CaO  |                 |            |                |            | **              | **         | **         |                    |                | **         | **         |                    |
| CaK <sub>2</sub> CO <sub>3</sub>                               |                 |            |                |            | *               | *          | *          | *                  |                |            |            |                    |
| K <sub>2</sub> Mg <sub>2</sub> (SO <sub>4</sub> ) <sub>3</sub> |                 | *          |                | *          |                 |            |            |                    |                |            |            |                    |
| MgO  |                 |            |                |            |                 |            |            |                    | *              | **         |            |                    |
| Ca <sub>2</sub> Mg(Si <sub>2</sub> O <sub>7</sub>              |                 | **         |                | *          |                 |            |            |                    |                |            |            |                    |
| KCl  |                 |            |                |            | *               | *          |            |                    | *              | *          | *          |                    |
| K <sub>2</sub> SO <sub>4</sub>                                 |                 |            |                |            | **              | ***        |            |                    | **             | ***        |            |                    |



33  
34  
35  
36  
37

**Figure 1.** Fraction of fuel ash that forms slag during the combustion of barley straw and barley husk pellets with and without addition of calcium lignosulfonate and marble sludge.



48  
49  
50  
51  
52  
53  
54  
55  
56  
57  
58  
59  
60

**Figure 2.** Slag samples collected from combustion of (a) barley straw pellets, (b) + 3 wt % calcium lignosulfonate, (c) barley husk pellets, (d) + 3 wt % calcium lignosulfonate.

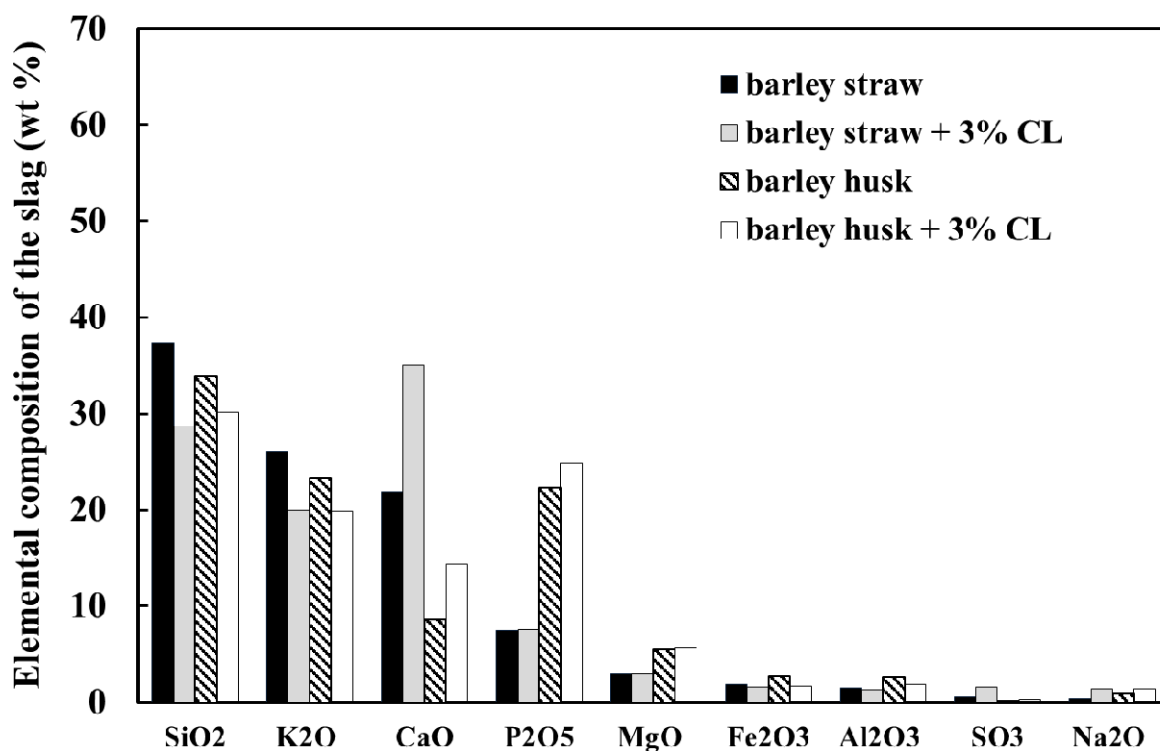
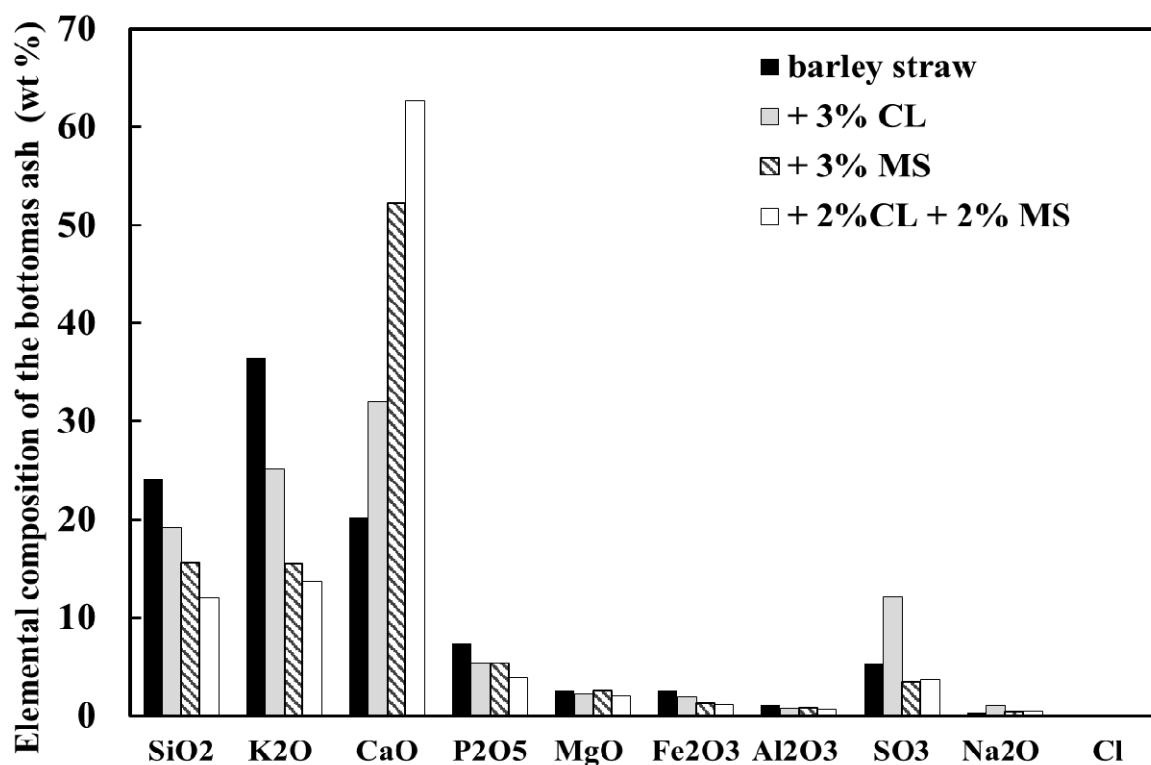
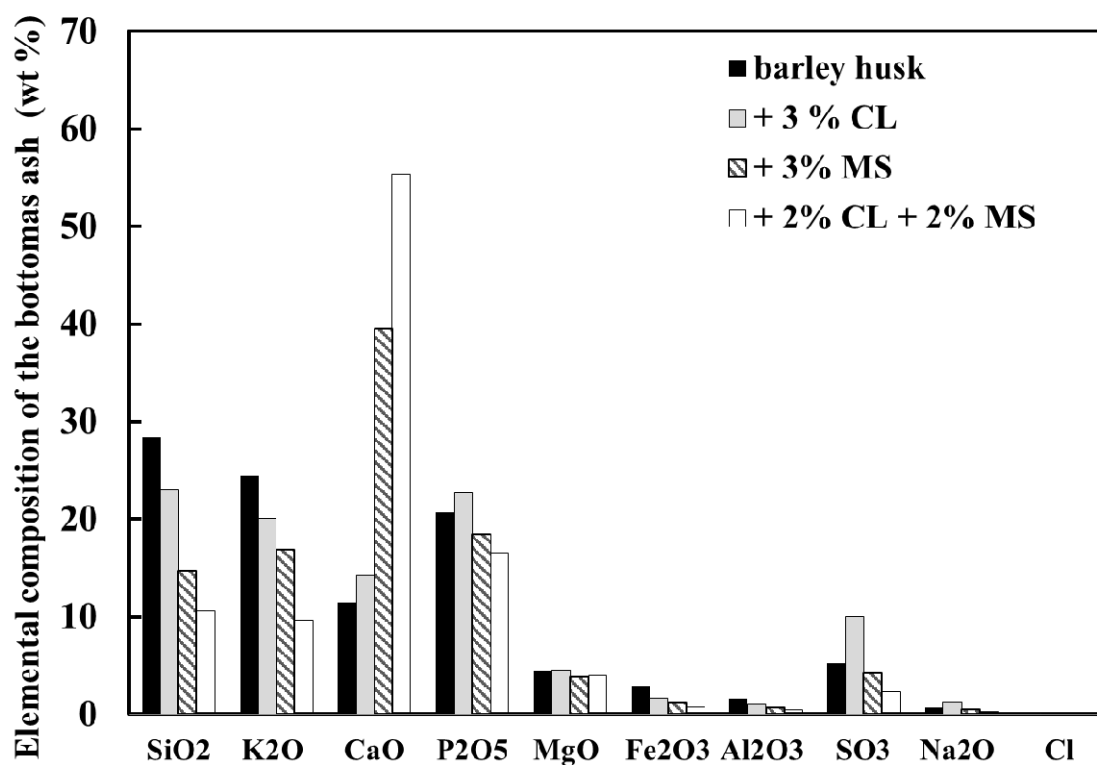


Figure 3. Elemental compositions (given as oxides) of the formed slag samples



**Figure 4.** Elemental compositions (given as oxides) of the formed bottom ash from combustion of barley straw with and without additive addition





**Figure 5.** Elemental compositions (given as oxides) of the formed bottom ash from combustion of barley husk with and without additive addition

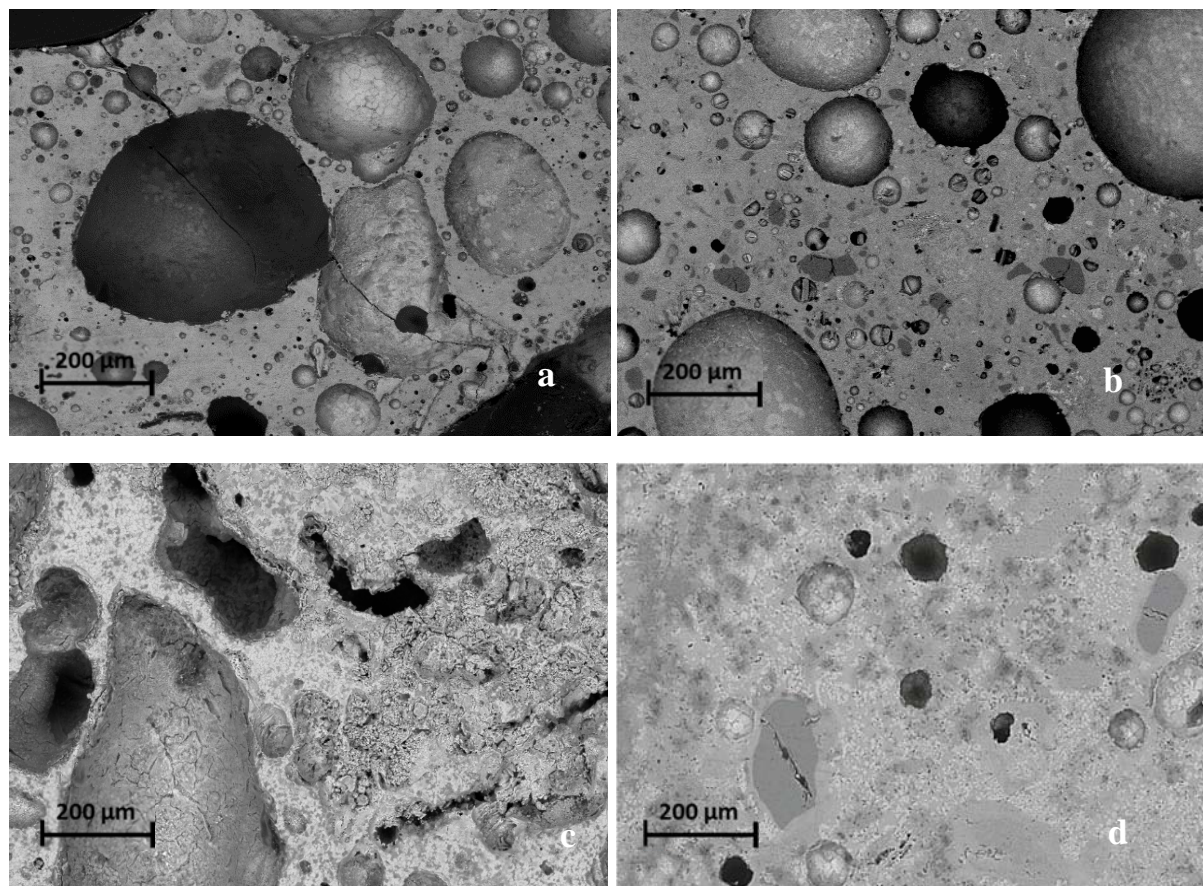
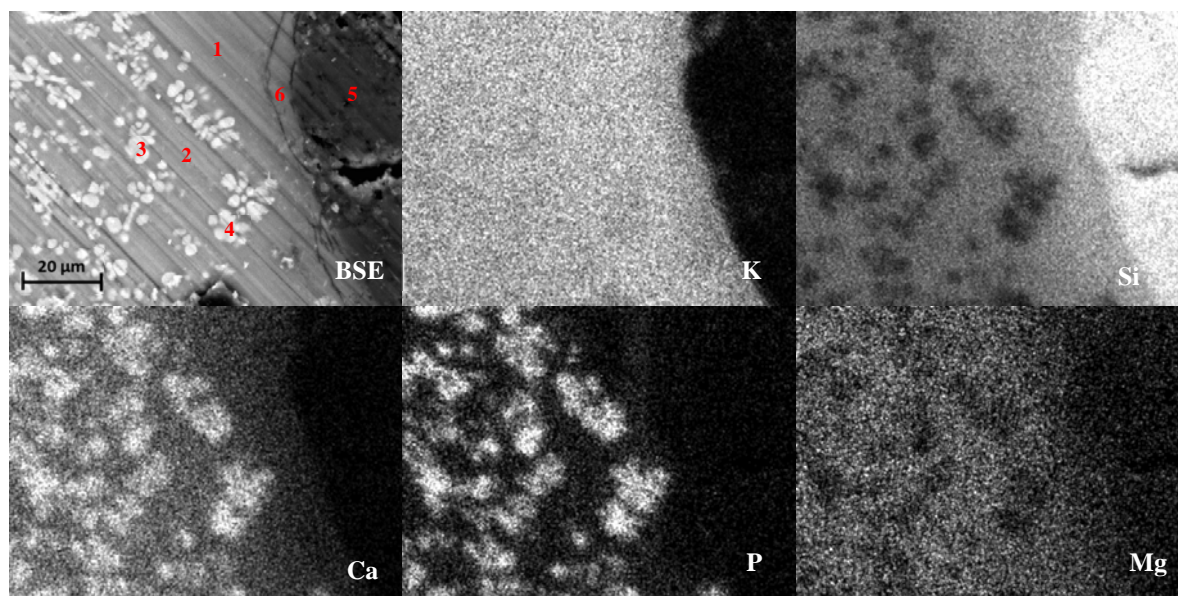
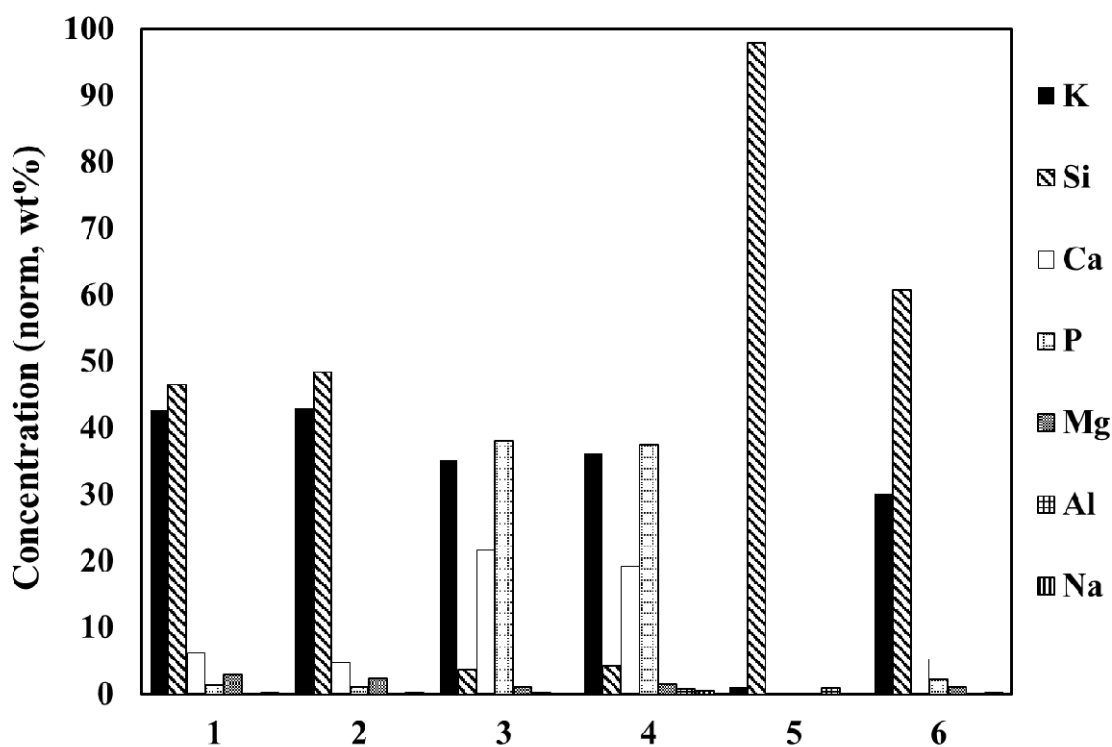


**Figure 6.** Back-scattered electron image of typical polished cross-section of slag samples from combustion of barley straw and barley husk pellets with and without additives: (a) barley straw, (b) barley husk, (c) barley straw + 3% calcium lignosulfonate and (d) barley husk + 3% calcium lignosulfonate



26  
27  
28  
29

**Figure 7.** Back-scattered electron image and elements mapping of slag sample formed during the combustion of barley straw pellets



55  
56  
57  
58  
59  
60

**Figure 8.** Element composition on C- and O-free basis of slag collected from combustion of barley straw pellets (marked spots in Figure 7)

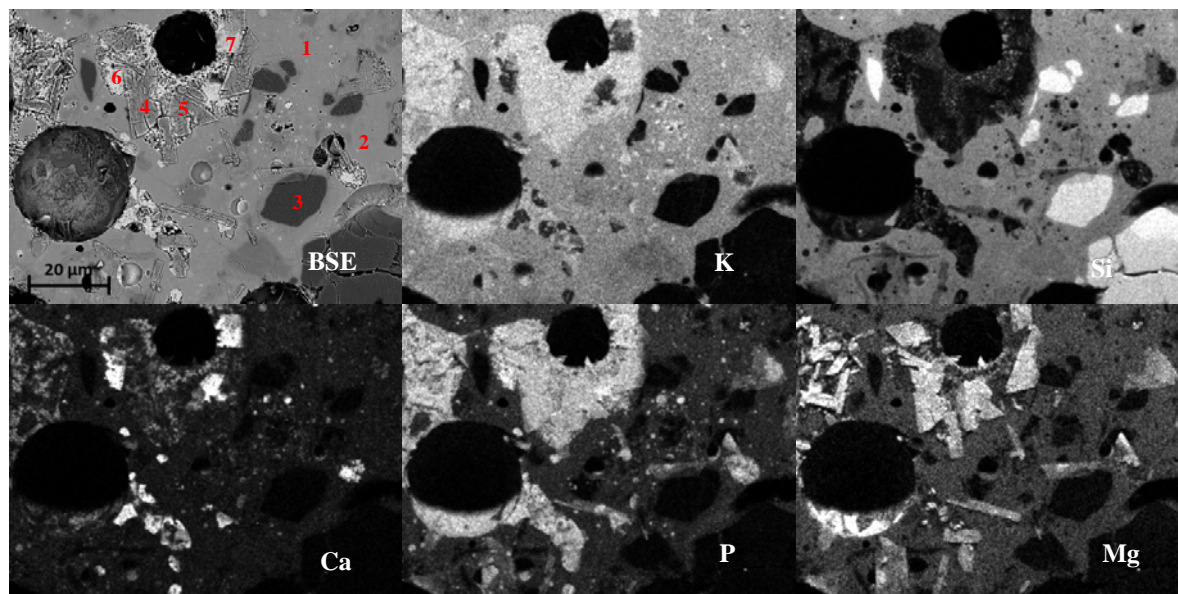


Figure 9. Back-scattered electron (BSE) image and elements mapping of slag sample formed during the combustion of barley husk pellets

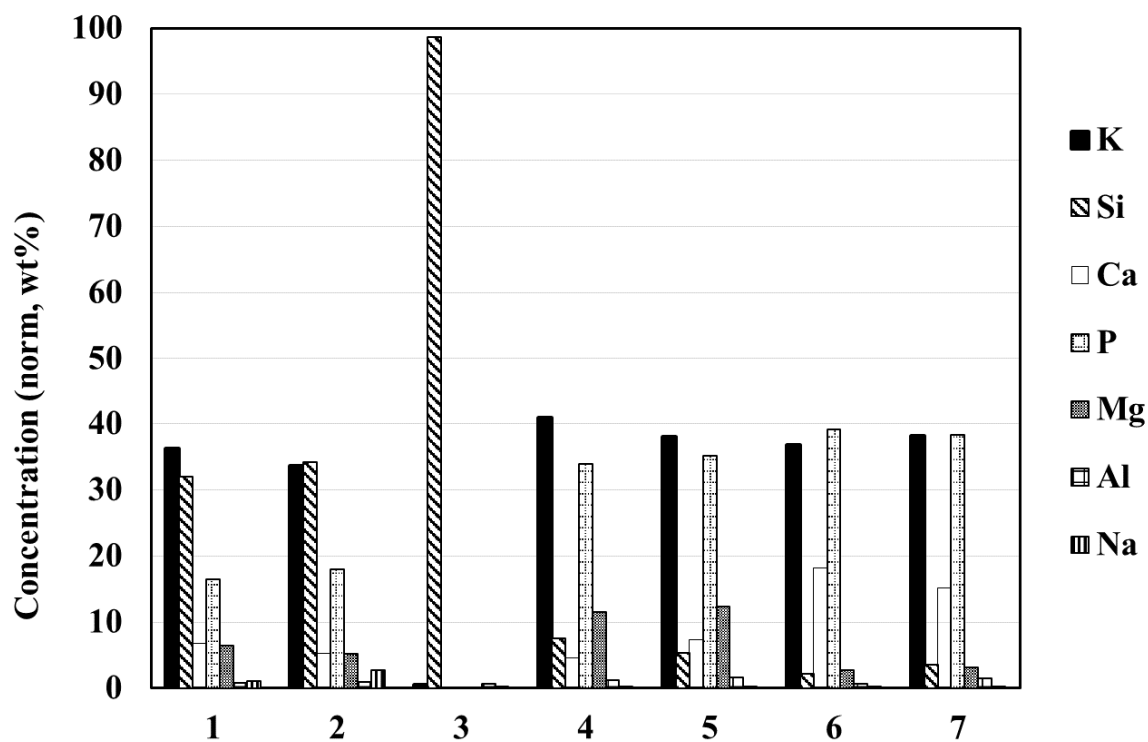
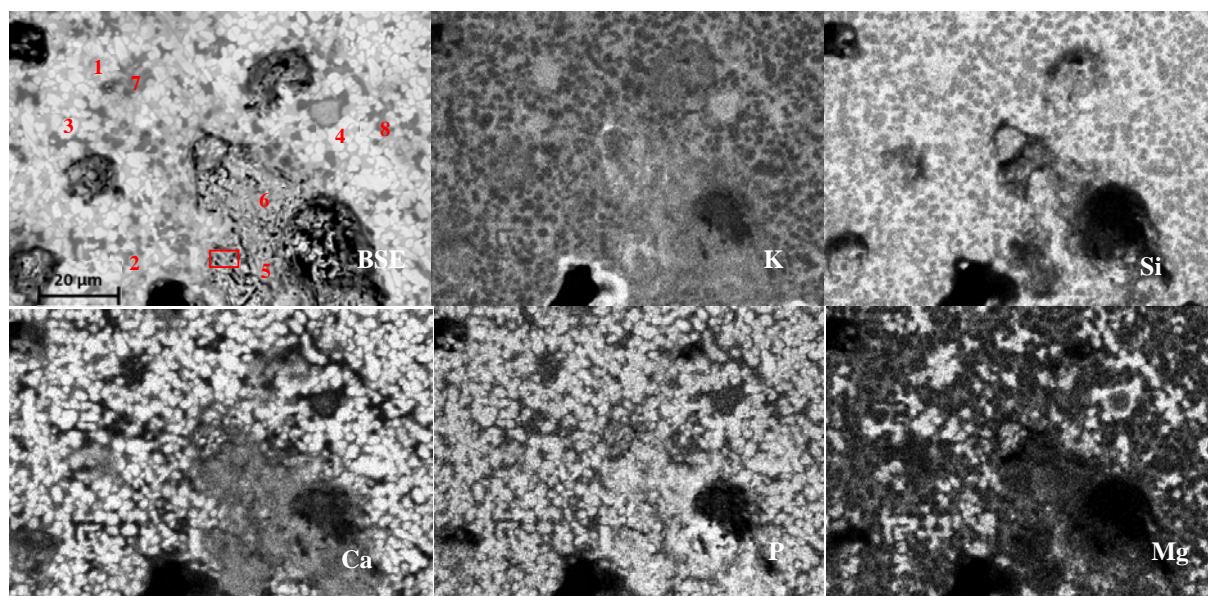
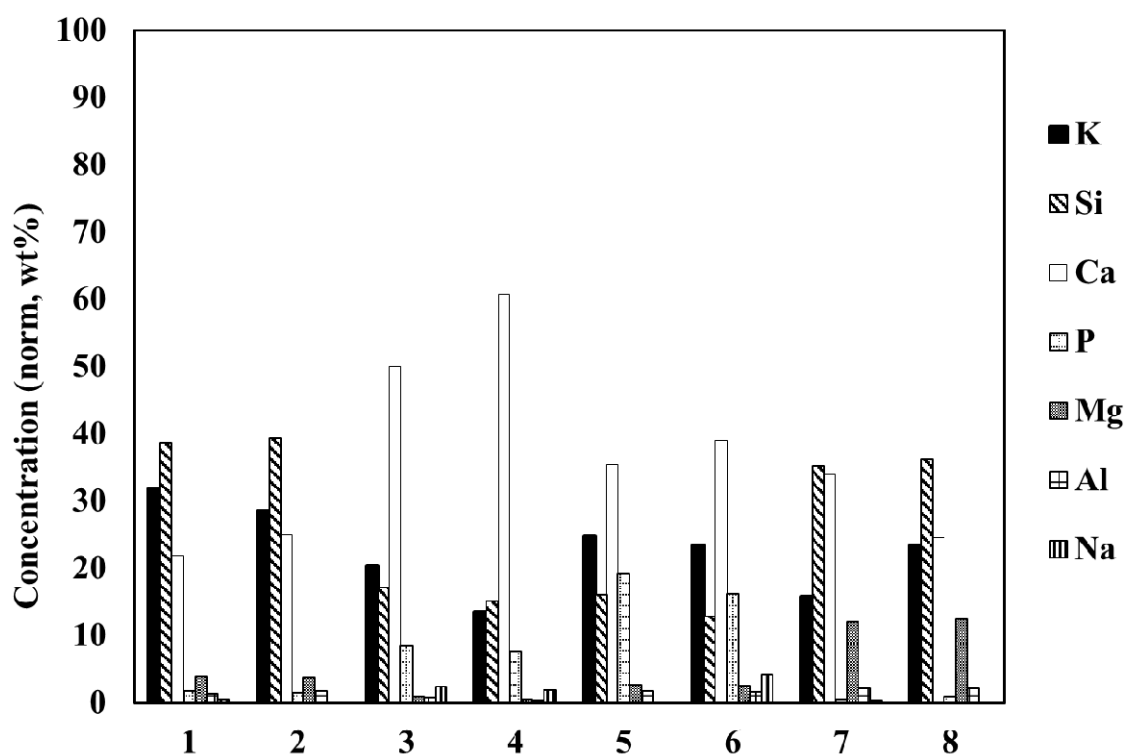


Figure 10. Element composition on C- and O-free basis of slag collected from combustion of barley husk pellets (marked spots in Figure 9)



**Figure 11.** Back-scattered electron (BSE) image and elements mapping of slag sample formed during the combustion of barley straw with and without additive addition



**Figure 12.** Element composition on C- and O-free basis of slag collected from combustion of barley straw pellets with addition of 3 % calcium lignosulfonate (marked spots in Figure 11)

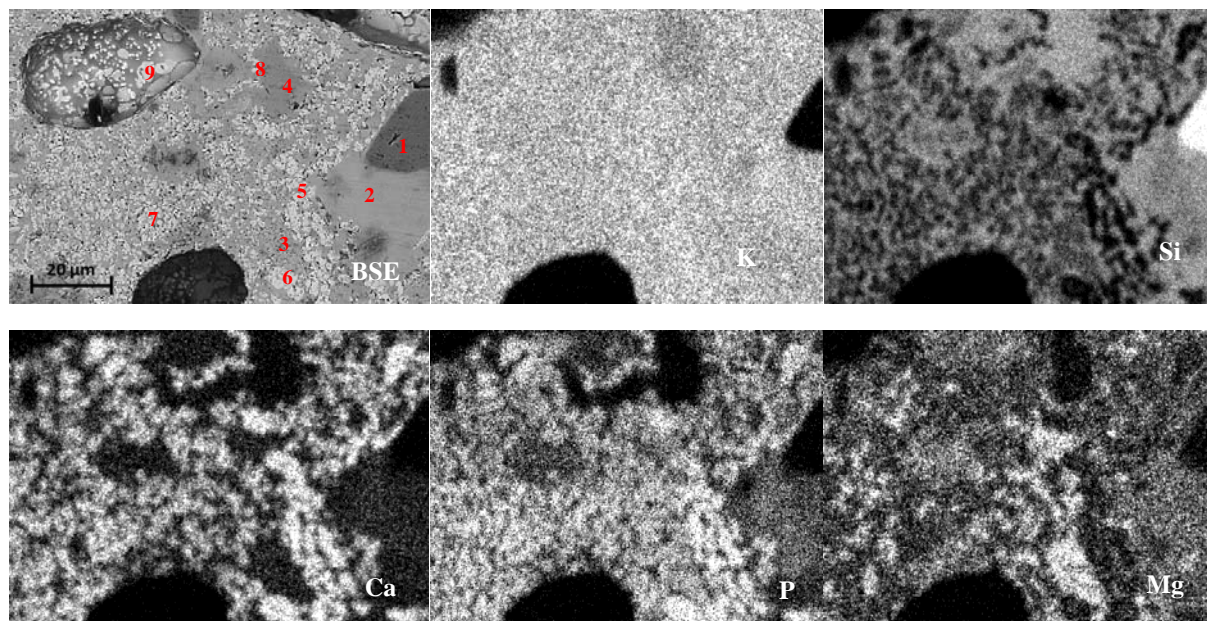


**Figure 13.** Back-scattered electron (BSE) image and elements mapping of slag sample formed during the combustion of barley husk pellets addition of 3 % calcium lignosulfonate

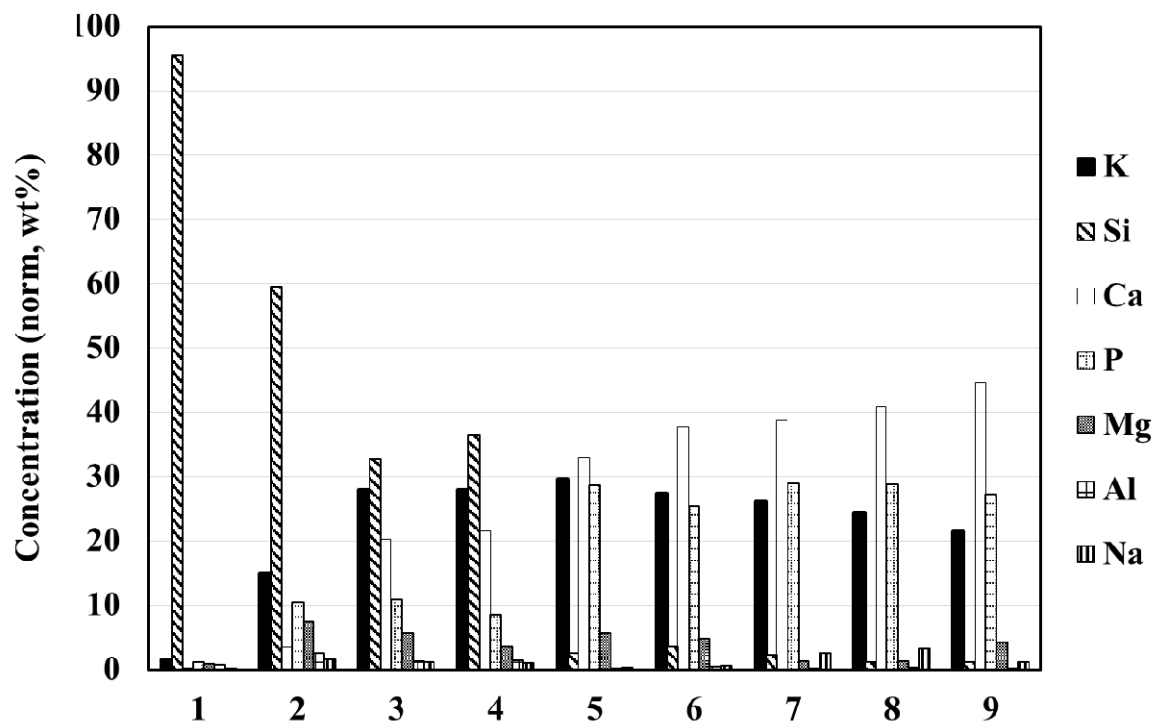


**Figure 14.** Element composition on C- and O-free basis of slag collected from combustion of barley husk pellets with addition of 3 % calcium lignosulfonate (marked spots in Figure 13)